Nuclide identification of radioactive sources from gamma spectra using artificial neural networks

N.P. Barradas[1], A. Vieira[2], M. Felizardo[1], M. Matos[3]
[1] Department of Nuclear Sciences and Engineering, Instituto Superior Técnico, Lisbon University, Portugal
[2] Medgical.AI, Portugal
[3] International Atomic Energy Agency
e-mail: nunoni@ctn.tecnico.ulisboa.pt

In principle, the analysis of gamma ray spectra for identifying the radionuclides present is a straightforward task, given that the gamma ray energies for each radionuclide are well known. In practice, there are several difficulties when using gamma spectroscopy of unknown samples, where it is a priori unknown how many and which radionuclides are present, and is what the internal configuration of the sample. In this work, 110 gamma ray spectra were measured, involving combinations of up to 10 different sources with different shielding and different measurement conditions: ^{22}Na, ^{57}Co, ^{60}Co, ^{88}Y, ^{109}Cd, ^{133}Ba, ^{137}Cs, ^{152}Eu, ^{204}Tl, ^{241}Am. Single source spectra were used to generate synthetic data using data augmentation techniques to address the issue of limited sample size. An ANN was trained using the synthetic data, and then applied to the analysis of the experimental multiple-source spectra. We report on the results, which show effective nuclide identification of radioactive sources from gamma spectra using ANNs.

1. Introduction

In principle, the analysis of gamma ray spectra for identifying the radionuclides present is a straightforward task, given that the gamma ray energies for each radionuclide are well known. In practice, there are several difficulties when using gamma spectroscopy of unknown samples, where it is a priori unknown how many and which radionuclides are present, and what is the internal configuration of the sample, including possible shielding. This is often the situation in radiological and nuclear security applications [1],[2]. Some of those difficulties are:

1. The intensities of gamma ray lines can be very different for the different radionuclides, as mixture of high intensity and low intensity sources is often present in one given sample.
2. Shielding attenuates different gamma rays differently, which affects the intensity of all gamma ray lines, but also affects the line ratio in radionuclides with more than one significant gamma ray. In nuclear security applications, shielding is often unknown, and these attenuations cannot be calculated a priori, which makes theoretical calculation of intensities very challenging.
3. Some radionuclides may be near or below the limit of detection (LOD). In cases where all gamma ray intensities of a radionuclide are below the LOD, no software or data analysis procedure can help; when at least one gamma ray is above, albeit near, the LOD, conventional data analysis techniques have difficulties in identifying the given radionuclide in an automated way.

Artificial Neural Networks (ANNs) are particularly suited to the analysis of complex data due to their superior pattern recognition capabilities. We have previously shown how ANNs can be efficiently developed to analyse neutron activation analysis data, which is based on gamma spectroscopy, performing as well as state of the art data analysis methods based on first principles [3]. Different machine learning methods, including ANNs, have also been applied to gamma spectroscopy [4]-[11]. These studies were conducted either using synthetic data without testing on experimental data, or testing on a very small amount of

experimental data. Most of the studies were conducted on single sources, i.e., on identification of the one single radionuclide present. One study used 1951 experimental single source data sets [10].

In this work, 110 gamma ray spectra were measured, involving combinations of up to 10 different sources with different shielding and different measurement conditions: ^{22}Na, ^{57}Co, ^{60}Co, ^{88}Y, ^{109}Cd, ^{133}Ba, ^{137}Cs, ^{152}Eu, ^{204}Tl, ^{241}Am. Single source spectra were used to generate synthetic data using data augmentation techniques to address the issue of limited sample size. An ANN was trained using the synthetic data, and then applied to the analysis of the experimental multiple-source spectra. We report on the results, which show effective nuclide identification of radioactive sources from complex multi-source gamma spectra using ANNs.

2. Experimental data

The experimental setup consisted of 1.5×1.5 in. $LaBr_3$(Ce) scintillation crystal in a hermetically sealed aluminium housing, including a photomultiplier tube, an internal magnetic/light shield, and a 14-pin connector. The detector has been combined with the Osprey®-DTB all-in-one HVPS, preamplifier, and digital MCA. The applied high voltage was 600 V, the rise time 1 μs and the range went to 2.6 MeV with 1024 channels. The resolution of the system was 3.6% at 662 keV (^{137}Cs FWHM). The instrument did not perform as well as a new device as it has been used in numerous applications previously. The scintillation material has a background that includes an intrinsic internal decay from the primordial radioisotope ^{138}La. This setup allowed to imitate more realistic data similar to results that Front Line Officers would obtain instead of sterile laboratory conditions.

Over the duration of 6 months (25.8.2023 - 14.2.2024) 110 spectra have been recorded. Various combinations of following sources have been used (activity on 25.8.2023) ^{204}Tl (6.32×10^4 Bq), ^{137}Cs (5.66×10^5 Bq), ^{60}Co (3.24×10^5 Bq), ^{57}Co (6.43×10^3 Bq), ^{109}Cd (1.11×10^4 Bq), ^{152}Eu (4.08×10^5 Bq), ^{88}Y (4.95×10^2 Bq), ^{241}Am (4.64×10^5 Bq), ^{133}Ba (3.94×10^5 Bq), and ^{22}Na (1.44×10^5 Bq). To match various levels of activities, the sources were placed at several distances, from the source-detector on contact (0 cm) to 10 cm. In few case we have also used Pb shielding of 2 or 5 mm. The background has been recorded several times. The background spectrum (Figure 1) illustrates the detection of X-rays, gamma and beta rays from the intrinsic decay of ^{138}La and alpha particles from the uranium decay chain, , in addition gamma rays from external natural ^{40}K [12]. The energy calibrations with ^{137}Cs, ^{60}Co, ^{88}Y, and ^{241}Am sources were repeated each month, the peaks with energies used for the calibrations are shown in Figure 2.

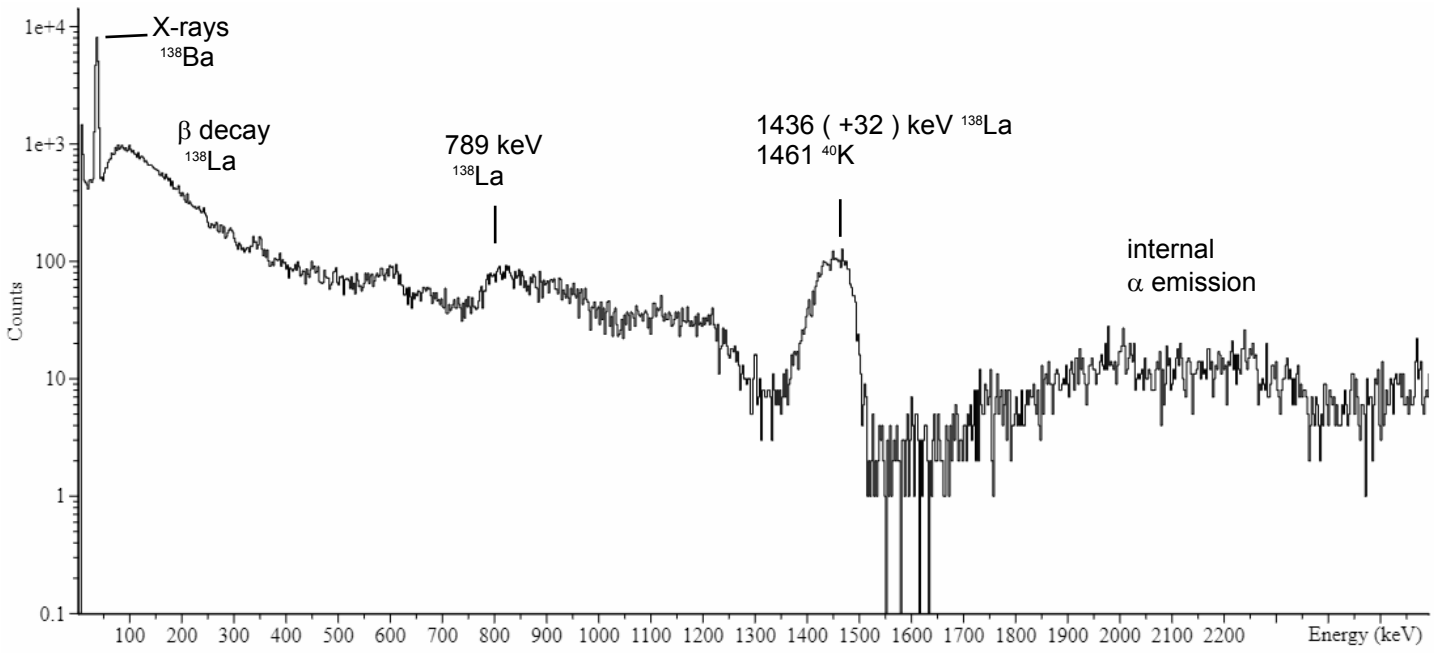

Figure 1. $LaBr_3(Ce)$ scintillation crystal spectrum of the background. Intrinsic radiation from ^{138}La and external radiation from ^{48}K can be detected.

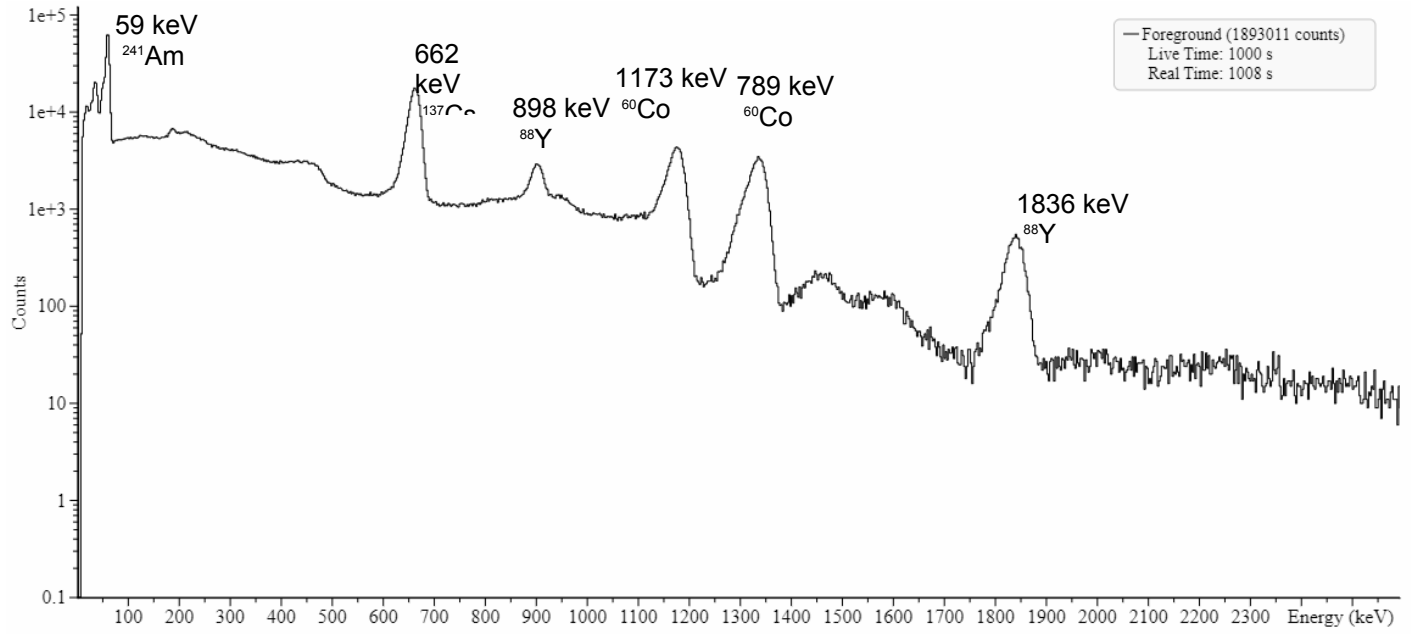

Figure 2. $LaBr_3(Ce)$ scintillation crystal energy calibration spectrum with ^{137}Cs, ^{60}Co, ^{88}Y, and ^{241}Am sources. This type of spectrum has also been used in further work.

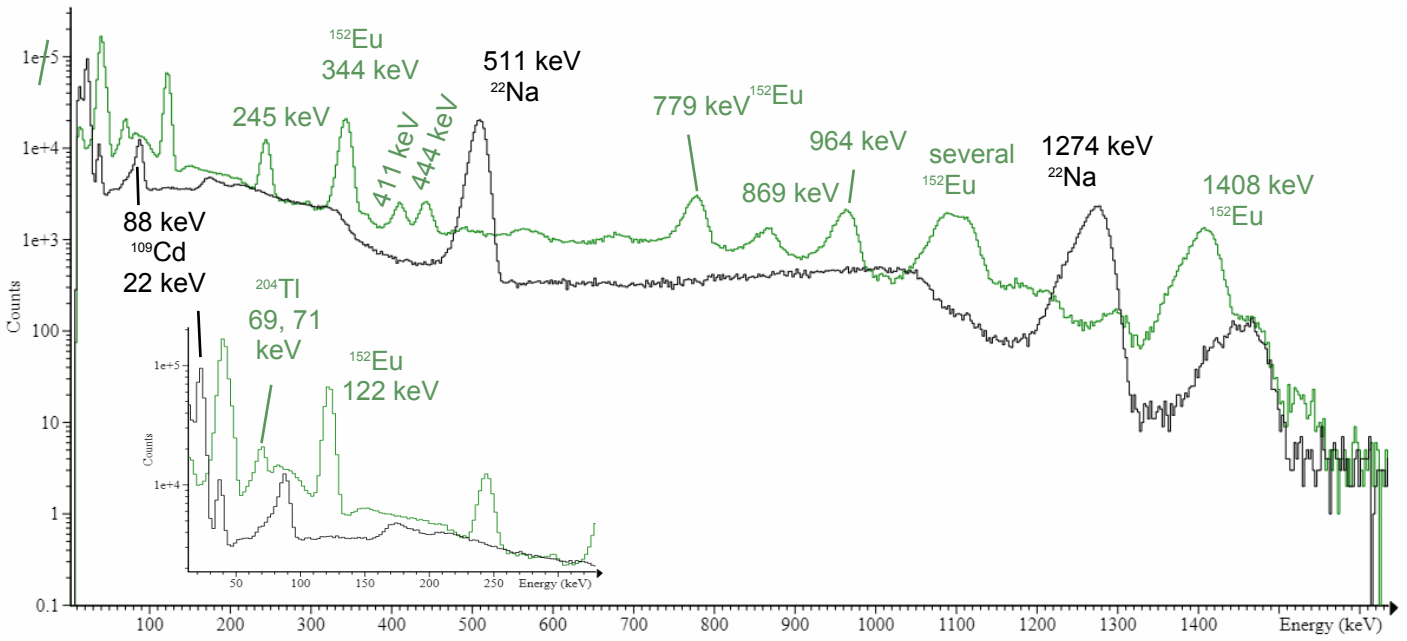

2024021402 2024021404 Cd109 Na22 Tl204 Eu152

3. Artificial Neural Networks

3.1 ANN architecture

For this work we used Convolutional Neural Networks (CNNs) [8]. CNNs are neural networks specifically designed for processing structured grid data. They are crucial for image processing because they adaptively learn spatial hierarchies of features through backpropagation, significantly enhancing tasks such as object detection, image classification, and segmentation. By leveraging convolutional layers, CNNs efficiently reduce the dimensionality of images while preserving essential features, leading to highly accurate and robust image analysis. The benefits of using 1D CNNs for Signal Analysis are:

1. **Automatic Feature Extraction**: Unlike traditional methods that require manual feature engineering, CNNs automatically learn features from the raw input data.
2. **Parameter Sharing**: Convolutional layers share parameters (weights) across different positions of the input, making the network more efficient and less prone to overfitting.
3. **Local Connectivity**: The use of kernels (w) helps in capturing local patterns within the input signal, which is crucial for understanding spectra data.
4. **Reduction in Computational Complexity**: By using pooling layers, the network reduces the dimensionality of the data, thus lowering the computational complexity, thus improving generalisation.

The convolution operation slides the kernel w across the input x , performing element-wise multiplications and summing them up along with the bias term to produce the output feature map y. In signal analysis, 1D CNNs are particularly effective because they can capture local dependencies and patterns in the data. For

instance, in a time-series dataset, patterns such as peaks, trends, and repetitive signals can be efficiently identified through the convolutional layers.

In our case, we fed the spectra (downsampled to 256 or 512 channels) using up to three 1D convolutional layers followed by maxpooling layers to introduce a computational bottleneck. To regularise the network we used L_2 regularisation on the dense layers. L2 regularization is a technique used in training neural networks to prevent overfitting, which occurs when a model performs well on training data but poorly on unseen data. It works by adding a penalty term to the loss function, which discourages the network from fitting the noise in the training data too closely - penalises large weights.

As loss function we used the binary cross-entropy (BCE), that is the most suitable for classification problems, given by the expression:

where y_{pred} are predictions and y_{true} are the real labels. The following describes the architecture of one kind of network tested. It is composed of a 1 dimensional convolutional layer (conv_1d) followed by a flatten layer (flatten_1), a dense layer with 30 neurons with the *gelu* activation function. Finally the output layer (layer_out) consists of 10 neurons (one for each nuclide) using a sigmoid activation.

Layer (type)	Output Shape	Parameters
input_c (InputLayer)	(None, 256, 1)]	0
conv1d_1 (Conv1D)	(None, 252, 100)	600
max_pooling1d_1	(None, 126, 100)	0
flatten_1 (Flatten)	(None, 3050)	0
layer2 (Dense)	(None, 30)	91530
layer_out (Dense)	(None, 10)	310

Total params: 117490 (458.95 KB)

We used Tensorflow Keras framework to build and train the network using the Adam optimizer [20]. We trained the network using 50 and 100 thousand synthetic spectra. From these examples, a random sample of 80% was used for the train set, i.e. these synthetic spectra were presented to the ANN with known outputs, and the remaining 20% were used for the test set, which are not directly used to train the ANN. Training was set to run up to 100 epochs or when the loss in the test set reaches an absolute minimum. Note that the output of the network are continuous values (from 0 to 1). To decide if a nuclide is present in the sample or not, we need to set a detection threshold level - in this case we took the obvious choice of 0.5. This threshold can be varied depending on the trade-off required between specificity and sensitivity. Since a few elements were hardest to detect, i.e. ^{57}Co, ^{109}Cd, ^{204}Tl, and ^{241}Am, we used a weighted loss function to put more emphasis in these radionuclides.

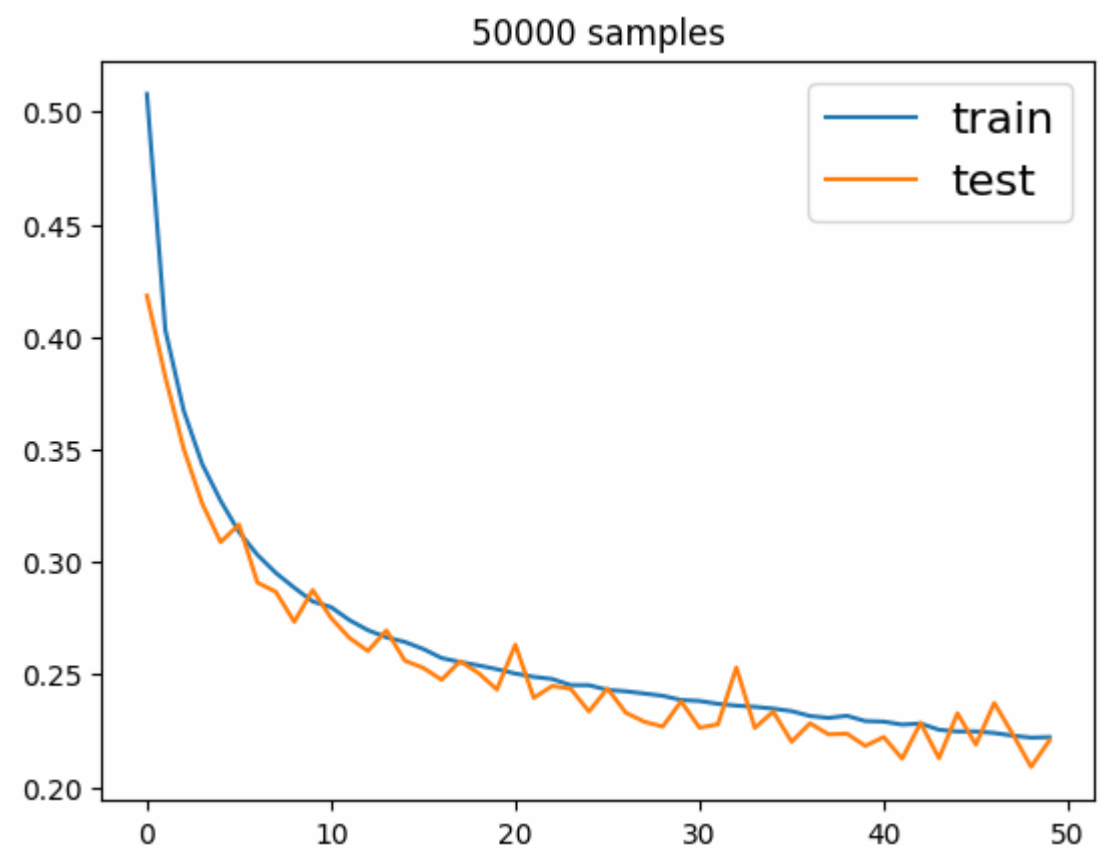

Figure: loss function for train and test set during training.

3.2 Synthetic data

ANNs usually require a large amount of training data. In the present problem, with a large number of inputs (the number of channels) and ten different outputs, the resulting ANNs have a very large number of connections and parameters, and the requirements for number of training data are consequently also very large. ANNs trained with limited amounts of data are prone to over-training, i.e., becoming specialized for the data they have been trained with, with limited capability of generalization to other cases. It is not feasible to measure a sufficient number of experimental spectra to train the ANN. Different approaches have been previously developed to tackle this issue. One approach, to use theoretically calculated data, has been used for techniques such as Rutherford backscattering [12], elastic backscattering [13], elastic recoil detection analysis [14], prompt gamma activation analysis [6], and gamma spectroscopy [11]. It has the advantage that any number of data, for any given experimental parameters, can be generated. One drawback is that the calculations can be very time-consuming, limiting the number of synthetic data that can be generated. Another potential drawback is that, if the theoretical calculation is not sufficiently realistic and accurate, the ANN will not be able to correctly analyse the experimental data. Another approach is to use a limited number of experimental data to generate synthetic data. This was successfully used in neutron activation analysis [3], which is also based on gamma spectroscopy, and was the option taken in this work.

Synthetic data were generated by linear combination of experimental data, after due consideration to pulse pileup was given. Pulse pileup is non-linear, and does not simply add when two sources are combined. In

other words, the pileup resulting from two sources being measured simultaneously is not equal (and in fact can be very different) to the sum of the pileup resulting from each source being measured separately. We addressed this by the following procedure: first, we used the algorithm by Molodtsov and Gurbich [15] to calculate the pileup in the experimental data. The algorithm depends on a few parameters, which were determined by analysing three experimental spectra measured explicitly for this purpose. These were from high activity sources at zero distance to the detector: ^{60}Co and ^{137}Cs first measured separately, and then measured together. Then, the parameters so determined were used to calculate the pileup for all other experimental data, which have much lower count rate and hence also much lower pileup. We subtracted the calculated pileup from the experimental data, obtaining pileup-free spectra. It is these pileup-free spectra that were combined linearly to form the synthetic data, which are therefore also pileup-free. The last step was to add calculated pileup to the synthetic data. This was done with the algorithm by Barradas and Reis [13], which produces results similar to that of Molodtsov and Gurbich when the count rate is not high; the main differences are that it does not include tail pileup, which is only significant for very high count rates, and that it is one to two orders of magnitude faster. The latter feature was determinant in the choice of using the Barradas and Reis algorithm for the synthetic data, given the very high number of synthetic spectra generated.

A restricted number of experimental data was selected to generate the synthetic data: only the 27 single source experimental data collected with the same livetime (1000 s) were used. This is not a principled restriction, and the code gives the user the option to use experimental data collected with more sources and with different livetime values. We call this set of 27 experimental data the "experimental training set". For each synthetic spectrum, a random number of spectra from the experimental training set was selected, from a minimum of 1 to a maximum of 10 for 40% of the synthetic spectra, and a maximum of 27 for the remainder. A (logarithmic) random factor from 10^{-2} to 10^{2} was used as multiplicative weight for each of the experimental spectra. A further (logarithmic) random factor from 10^{-2} to 10^{2} was used as multiplicative weight for the total yield with respect to the average yield of the selected experimental spectra. Additionally, 1% of the synthetic spectra were generated from background experimental spectra, collected without sources.

In this process, it is possible that a radionuclide that is visible above the limit of detection (LOD) in the original single source experimental spectrum, becomes invisible (i.e., below LOD) in the synthetic spectrum, because it is superimposed to a large background, or even a large peak, from a different radionuclide from one of the other original single source experimental spectra used to construct the synthetic spectrum. The code for generation of synthetic data checks, for each radionuclide in principle present, whether at least one of the respective gamma lines is above the LOD [17]. If not, the radionuclide is considered not to be present in the synthetic spectrum.

The experimental data had 1024 channels. This is a high number of inputs for an ANN, which leads to a very high number of parameters and, consequently, to difficulties in training the ANN efficiently and increases the risk of overfitting. In order to reduce the number of parameters, we compressed the synthetic spectra by grouping every four or every two channels thus reducing the number of channels to 256 or 512, respectively. The latter case, 512 channels, leads to an energy width of the compressed channels close to the FWHM energy resolution of the detector used, which should be sufficient to discriminate between neighbouring gamma lines in most cases.

4. Results and discussion

We compare the performance of the ANN with the Interspec software for peak analysis on 76 spectra. These are the 70 experimental spectra with two or more radionuclides present and acquisition time 1000 s, and six background spectra with acquisition time 1000.

We used two metrics: False Positive (FP), number of cases predicted as present when they are in fact absent and False Negatives (FN), number of cases predicted as not present when they are present in the sample. For InterSpec (IS) we can only calculate the FN. We can see that the ANN is capable to detect radionuclides in the samples with the same accuracy as humans using Interspec (IS), sometimes with a higher accuracy as is the case of Am-241 and Cd-109.

The false positives detected by the ANN can be attributed to the bias in the training data, which contains very few negative examples (only 1%) with background only. This imbalance causes the ANN to be overly sensitive to potential positives, increasing the likelihood of false alarms.

Table : results of ANN compared with Interspec software (IS) for the 70 samples with elements. FP is the false positives and FN false negatives.

Element	Total Positives	Total Negatives	FP (ANN)	FN (ANN)	FN (IS)
Co-60	25	45	0	0	0
Cs-137	26	44	0	0	0
Am-241	18	52	0	6	7
Y-88	21	49	0	4	4
Eu-152	21	49	1	0	0
Ba-133	15	55	0	0	0
Na-22	11	59	0	0	0
Co-57	11	59	4	4	4
Tl-204	10	60	5	3	3
Cd-109	29	41	2	13	16

Detail some cases of superposition (Ba and Cd)

Trace a AUC curve for classification of a specific element

False positives

Material	FP	FN
Co-60		
Cs-137		

Am-241		'data_000019','data_000020', 'data_000021','data_000026', 'data_000027','data_000063
Y-88		data_000046, data_000047 data_000048, data_000049
Eu-152	data_000081	
Ba-133		
Na-22		
Co-57	data_000028, data_000056, 'data_000091, data_000103	'data_000082, data_000083, 'data_000088, data_000093
Tl-204	['data_000047', 'data_000105', 'data_000106', 'data_000109']	['data_000099', 'data_000100', 'data_000103']
Cd-109	data_000046 data_000110	['data_000073', data_000074', 'data_000079', 'data_000080', 'data_000081', 'data_000082', 'data_000083', 'data_000084', 'data_000085', 'data_000086', 'data_000087', 'data_000088', 'data_000093']

5. Summary and outlook

Uranium

Confidence – use ANN quantitative output instead of 0/1; or refine with uncertainty LOD.

Conflict of Interest statement
The authors have no competing interests to declare that are relevant to the content of this article.

Funding acknowledgement
Received funding from IAEA Contract TAL-NSNS20231117-005, Nuclide identification of shielded radioactive sources from measured spectra using artificial neural networks.

References

[1] Kouzes R. Detecting Illicit Nuclear Materials. American Scientist. 2005;93(5):422. https://doi.org/10.1511/2005.55.422
[2] Runkle RC, Smith LE, Peurrung AJ. The Photon Haystack and Emerging Radiation Detection Technology. Journal of Applied Physics. 2009;106(4):041101. https://doi.org/10.1063/1.3207769
[3] N. Pessoa Barradas, N. Farjallah, A. Vieira, M. Blaauw, Journal of Radioanalytical and Nuclear Chemistry 332 (2023) 3421–3429. https://doi.org/10.1007/s10967-022-08568-8

[4] M. Kamuda, J. Stinnett, C. J. Sullivan, Automated Isotope Identification Algorithm Using Artificial Neural Networks, in IEEE Transactions on Nuclear Science 64 (2017) 1858-1864. https://doi.org/10.1109/TNS.2017.2693152 (train from synthetic, 5 sources selected from 32 RNs, a few experimental spectra, no stats on results)

[5] Jinhwan Kim, Kyung Taek Lim, Junhyeok Kim, Chang-jong Kim, Byoungil Jeon, Kyeongjin Park, Giyoon Kim, Hojik Kim, Gyuseong Cho, Quantitative analysis of NaI(Tl) gamma-ray spectrometry using an artificial neural network, Nuclear Instruments and Methods in Physics Research Section A 944 (2019) 162549. https://doi.org/10.1016/j.nima.2019.162549 (train from exp, 9 sources of which 6 present, superimposed, 6 experimental spectra)

[6] Bilton KJ, Joshi THY, Bandstra MS, et al, Neural Network Approaches for Mobile Spectroscopic Gamma-Ray Source Detection, J. Nucl. Eng. 2 (2021) 190–206. https://doi.org/10.3390/jne2020018 (synthetic only, single source)

[7] Bon Tack Koo, Hyun Cheol Lee, Kihun Bae, Yongkwon Kim, Jinhun Jung, Chang Su Park, Hong-Suk Kim, Chul Hee Min, Development of a radionuclide identification algorithm based on a convolutional neural network for radiation portal monitoring system, Radiation Physics and Chemistry 180 (2021) 109300. https://doi.org/10.1016/j.radphyschem.2020.109300 (train from exp, 4 sources, single, rad portal)

[8] Géron, A.. Hands-On Machine Learning with Scikit-Learn, Keras, and TensorFlow: Concepts, Tools, and Techniques to Build Intelligent Systems (2022). O'Reilly Media.

[9] D. Pérez-Loureiro, J. Alexander, Radioisotope identification using CLYC detectors, 21st IEEE International Conference on Machine Learning and Applications (Nassau, Bahamas) (2022). https://doi.org/10.1109/ICMLA55696.2022.00214(train from 1951 experimental single source)

[10] Mark S. Bandstra, Joseph C. Curtis, James M. Ghawaly Jr, A. Chandler Jones, Tenzing H. Y. Joshi, Explaining machine-learning models for gamma-ray detection and identification, PLoS ONE 18 (2023) e02868292023. https://doi.org/10.1371/journal.pone.0286829 (train from synth, 25 single sources, no exp data)

[11] G. Harrison, J. Alexander, A. Erlandson, D. Godin, O. Kamaev, A. Maunsell, D. Pérez-Loureiro, E.T: Rand, D. Thakkar, M. Thompson, J. Woo, Modelling tools for enhancing nuclear security, ICONS 2024, International Conference on Nuclear Security: Shaping the Future, 20-24 May 2024, Vienna, Austria (preprint). (synthetic only, single source)

[12] D. Alexiev, L. Mo, D. Prokopovich, M. Smith, M. Matuchova, (2008). Comparison of and With NaI(Tl) and Cadmium Zinc Telluride (CZT) Detectors. Nuclear Science, IEEE Transactions on. 55. 1174 - 1177. 10.1109/TNS.2008.922837.

[13] J. Li, J. Alexander, M. Echlin, K. Stoev, M. Thompson, Advancing isotope identification algorithms for mid-resolution detectors, ICONS 2024, International Conference on Nuclear Security: Shaping the Future, 20-24 May 2024, Vienna, Austria (preprint). (synthetic training, 4 sources, single sources, 4x8 exp spectra)

[14] Pessoa Barradas N, Vieira A (2000) Artificial neural network algorithm for analysis of Rutherford backscattering data. Phys Rev E 62:5818–5829. DOI https://doi.org/10.1103/PhysRevE.62.5818

[15] Vieira A, Pessoa Barradas N (2001) Composition of NiTaC films on Si using neural networks analysis of elastic backscattering data. Nucl Instrum Methods Phys Res B 174:367–372. DOI https://doi.org/10.1016/S0168-583X(00)00621-2

[16] Nené NR, Vieira A, Pessoa Barradas N (2006) Artificial neural network analysis of RBS and ERDA spectra of multilayered multielemental samples. Nucl Instrum Methods Phys Res B 246:471–478. DOI https://doi.org/10.1016/j.nimb.2006.01.016

[17] L. Molodtsov, A. F. Gurbich, Nucl. Instru, Method. Phys. Res. B 267 (2009) 3484-3487. https://doi.org/10.1016/j.nimb.2009.08.008
[18] N. P. Barradas, M. Reis, X-Ray Spectrometry 35 (2006) 232-237. https://doi.org/10.1002/XRS.903
[19] J. L. Alvarez, Health Physics 93 (2007) 120-126. https://doi.org/10.1097/01.hp.0000261331.73389.bd
[20] Kingma, Diederik, and Ba, Jimmy. "Adam: A Method for Stochastic Optimization." International Conference on Learning Representations (ICLR), 2015, San Diego, CA, USA.
[21]